nature neuroscience

HDAC-mediated deacetylation of NF-κB is critical for Schwann cell myelination

Ying Chen[1,2], Haibo Wang[1], Sung Ok Yoon[3], Xiaomei Xu[1], Michael O Hottiger[4], John Svaren[5], Klaus A Nave[6], Haesun A Kim[7], Eric N Olson[2] & Q Richard Lu[1,2]

Schwann cell myelination is tightly regulated by timely expression of key transcriptional regulators that respond to specific environmental cues, but the molecular mechanisms underlying such a process are poorly understood. We found that the acetylation state of NF-κB, which is regulated by histone deacetylases (HDACs) 1 and 2, is critical for orchestrating the myelination program. Mice lacking both HDACs 1 and 2 (HDAC1/2) exhibited severe myelin deficiency with Schwann cell development arrested at the immature stage. NF-κB p65 became heavily acetylated in HDAC1/2 mutants, inhibiting the expression of positive regulators of myelination and inducing the expression of differentiation inhibitors. We observed that the NF-κB protein complex switched from associating with p300 to associating with HDAC1/2 as Schwann cells differentiated. NF-κB and HDAC1/2 acted in a coordinated fashion to regulate the transcriptionally linked chromatin state for Schwann cell myelination. Thus, our results reveal an HDAC-mediated developmental switch for controlling myelination in the peripheral nervous system.

Myelination of axons by Schwann cells in the peripheral nervous system (PNS) is essential for axonal insulation and saltatory conduction of action potentials. Peripheral myelin defects underlie various inherited or acquired demyelinating neuropathies in the PNS, leading to motor and sensory disabilities[1]. Schwann cell myelination is a complex developmental process, with a different set of regulators being sequentially induced to drive successive transitions until mature myelin is formed. Recent studies have revealed a transcriptional cascade that positively and negatively controls Schwann cell differentiation in a spatiotemporally specific manner[2,3]. Given that expression of these factors is regulated by different environmental cues, it is conceivable that epigenetic mechanisms are important for instructing the myelination program. A well-studied mechanism of chromatin remodeling is mediated by histone methylation and acetylation, the latter being dynamically controlled by histone acetyltransferases (HATs) and HDACs[4]. Recently, HDAC1 and HDAC2 were shown to be essential for CNS myelination[5,6]; however, their function and underlying mechanisms in Schwann cell differentiation and myelination remain elusive.

RESULTS

To define the role of HDAC1 and HDAC2 in Schwann cell development, we generated Cre-mediated *Hdac1* and *Hdac2* deletion mutant mice (*Hdac1*$^{loxP/loxP}$*; Dhh-cre* and *Hdac2*$^{loxP/loxP}$*; Dhh-cre*) and a double knockout mutant (*Hdac1*$^{loxP/loxP}$*; Hdac2*$^{loxP/loxP}$*; Dhh-cre*, dCKO) mouse. In these mice, *Hdac1* and *Hdac2* were flanked by *loxP* sites and *cre* was driven by the *Dhh* promoter, resulting in the deletion of the *Hdac1* and *Hdac2* genes in cells of the Schwann cell lineage[7]. *Hdac1* and *Hdac2* single mutants appeared to be normal compared to heterozygous control littermates, whereas dCKO mice developed severe tremors, hindlimb paralysis and died around postnatal week 2 (**Supplementary Fig. 1**).

The sciatic nerves isolated from dCKO mice at postnatal day 7 (P7) appeared to be much thinner and translucent compared with the control and *Hdac1* or *Hdac2* single mutants (**Fig. 1a**). Electron microscopy ultrastructural analysis revealed that there was a severe myelin deficit in dCKO mice and that the majority of Schwann cells appeared to be associated with multiple axon bundles, but did not form myelin sheaths around axons (**Fig. 1a**). Similarly, at P0, the majority of Schwann cells failed to establish a 1:1 relationship with individual axons, although a few Schwann cells were able to sort the axons (**Fig. 1b**). The absence of a discernable myelination defect in *Hdac1* or *Hdac2* single mutants suggests that these HDACs function redundantly during Schwann cell differentiation. Consistently, we observed upregulation of HDAC2 or HDAC1 in *Hdac1*$^{loxP/loxP}$*; Dhh-cre* and *Hdac2*$^{loxP/loxP}$*; Dhh-cre* sciatic nerves, respectively (**Fig. 1c**), suggesting that each has a compensatory effect in the other's absence. As *Hdac1* or *Hdac2* single mutant phenotypes were indistinguishable from that of the heterozygous control, we focused on the control (*Hdac1*$^{loxP/+}$*; Hdac2*$^{loxP/+}$*; Dhh-cre*) and dCKO mice for subsequent analyses. Consistent with our electron microscopy analysis, expression of mature myelin components, such as Mbp, Mag and Mpz, was

[1]Department of Developmental Biology and Kent Waldrep Foundation Center for Basic Neuroscience Research on Nerve Growth and Regeneration, University of Texas Southwestern Medical Center, Dallas, Texas, USA. [2]Molecular Biology, University of Texas Southwestern Medical Center, Dallas, Texas, USA. [3]Department of Molecular and Cellular Biochemistry, Center for Molecular Neurobiology, Ohio State University, Columbus, Ohio, USA. [4]Institute of Veterinary Biochemistry and Molecular Biology, University of Zurich, Zurich, Switzerland. [5]Department of Comparative Biosciences and the Waisman Center, University of Wisconsin, Madison, Wisconsin, USA. [6]Max Planck Institute of Experimental Medicine, Department of Neurogenetics, Goettingen, Germany. [7]Department of Biological Sciences, Rutgers University, Newark, New Jersey, USA. Correspondence should be addressed to Q.R.L. (qrichard.lu@utsouthwestern.edu).

Received 12 November 2010; accepted 18 February 2011; published online 20 March 2011; doi:10.1038/nn.2780

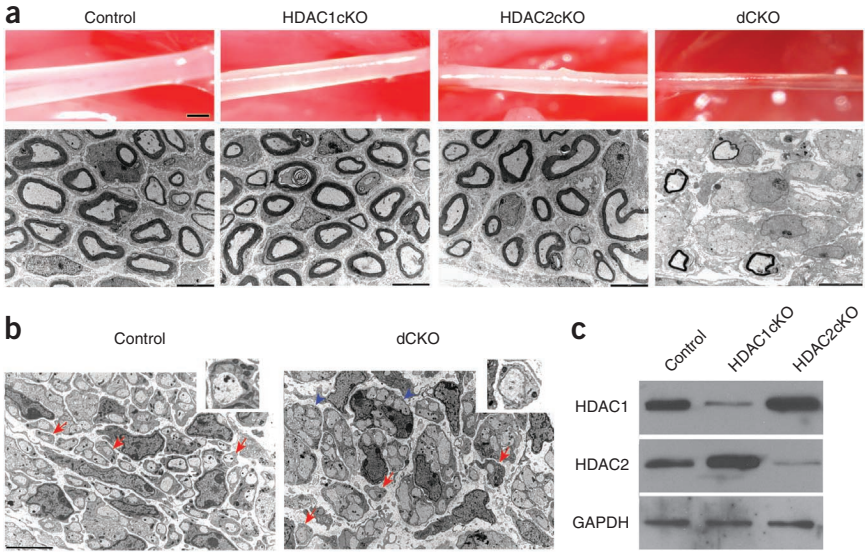

Figure 1 Ablation of HDAC1 and HDAC2 in the Schwann cell lineage results in severe myelination defects in sciatic nerves. (**a**) Appearance (upper panel) and electron microscopy analysis (lower panel, cross-section) of sciatic nerves from control and HDAC1cKO (*Hdac1*$^{loxP/loxP}$; *Dhh-cre*), HDAC2cKO (*Hdac2*$^{loxP/loxP}$; *Dhh-cre*) and dCKO mutants at P7. (**b**) Electron microscopy analysis of cross sections of control and dCKO sciatic nerves at P0. Inserts are shown for an individual sorted axon (arrows). Arrowheads indicate unsorted axons. (**c**) Western blot analysis of HDAC1 and HDAC2 expression using sciatic nerves from control, HDAC1cKO and HDAC2cKO at P4. GAPDH as a loading control. Full-length blots and gels are shown in **Supplementary Figure 6**. Scale bars represent 1 mm (**a**, top) 5 μm (**a**, bottom, and **b**).

significantly downregulated in dCKO sciatic nerves (**Fig. 2**), indicating that there was a severe defect in Schwann cell differentiation. In contrast, the number of immature Schwann cells expressing S100β and p75 was comparable to the control at P4 (**Fig. 2a**) and their proliferation was unaffected on the basis of Ki67 expression and BrdU incorporation (**Supplementary Fig. 2a**,**b**). There was a slight increase in the percentage of apoptotic cells in the nerves (**Supplementary Fig. 2c**); however, it did not alter the overall number of immature Schwann cells. These results suggest that Schwann cell development becomes arrested at the immature stage in the absence of HDAC1 and HDAC2.

Because Schwann cell development is controlled by a series of positive and negative regulatory factors[2,3], we next measured the mRNA levels of these regulators. In dCKO sciatic nerves, we observed not only a significant reduction in expression of positive regulators, including *Oct6* (also known as *Scip* and *Pou3f1*), *Sox10*, *Krox20* (also known as *Egr2*) and *Gpr126*, but also a concomitant increase of negative regulators of Schwann cell differentiation, such as *Sox2*, *Sox11*, *Jagged1*, *Jun* (*c-Jun*), *Hes1*, *Hes5*, *Id2* and *Id4* (**Fig. 2c**). Protein levels of important Schwann cell differentiation regulators, such as Sox10, Oct6 and Krox20, were correlated with their mRNA levels, as determined by quantitative RT-PCR (qRT-PCR; **Fig. 2b**,**c**). These results suggest that HDAC1- and HDAC2-dependent epigenetic modifications control the overall transcriptional program to orchestrate proper Schwann cell differentiation.

Myelination deficiency in dCKO sciatic nerves suggests that HDAC1 and HDAC2 are likely to target critical transcription factors for Schwann cell differentiation. As a candidate molecule, we focused on NF-κB, as it is crucial for Schwann cell differentiation by regulating expression of key differentiation regulators such as Oct6 (ref. 8) and, in addition, its p65 subunit is known to undergo a reversible acetylation/deacetylation by HATs (for example, p300) and HDACs[9].

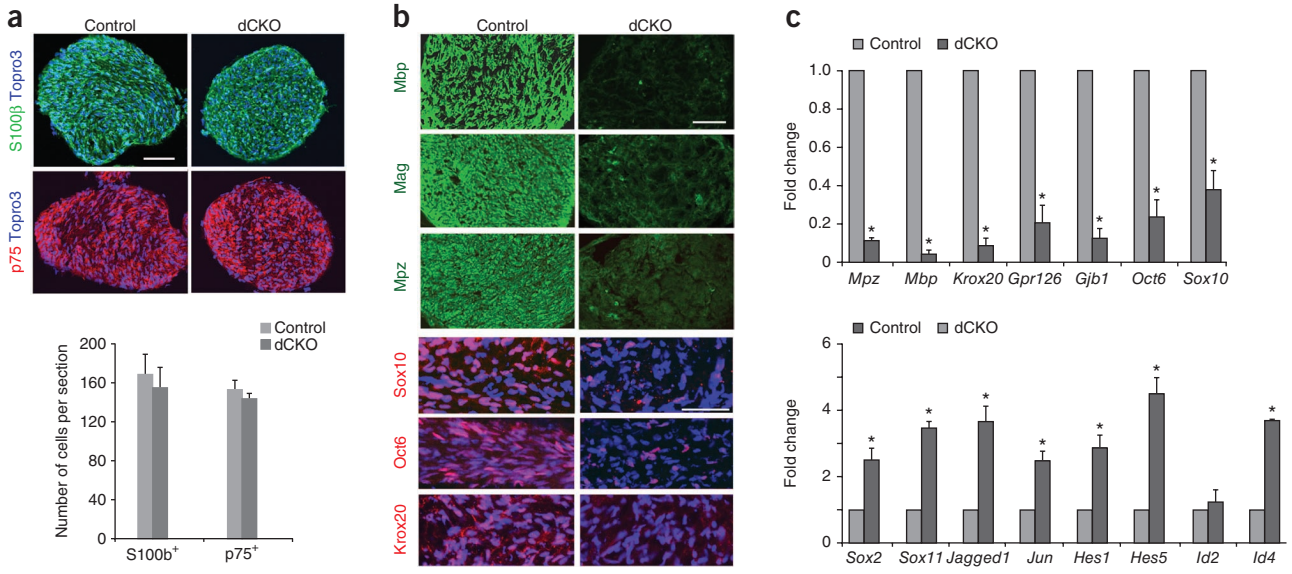

Figure 2 Effects of HDAC1 and HDAC2 deletion on Schwann cell precursor formation and differentiation. (**a**) Cross sections of sciatic nerves of control and dCKO mice at P4 were immunostained with antibodies to S100β and p75. Cell nuclei were counterstained with Topro3. Bottom, quantification of S100β-positive or p75-positive cells per cross-section. (**b**) Sciatic nerves of control and dCKO mice at P5 were immunostained with antibodies to myelin components (cross-sections) and transcriptional regulators (longitudinal sections) as indicated. (**c**) qRT-PCR analysis of myelin-associated genes, promyelinating transcriptional regulators (top) and negative regulators (bottom) in sciatic nerves of control and dCKO mice at P4 (* $P < 0.01$). Scale bars represent 60 μm (**a**) and 40 μm (**b**).

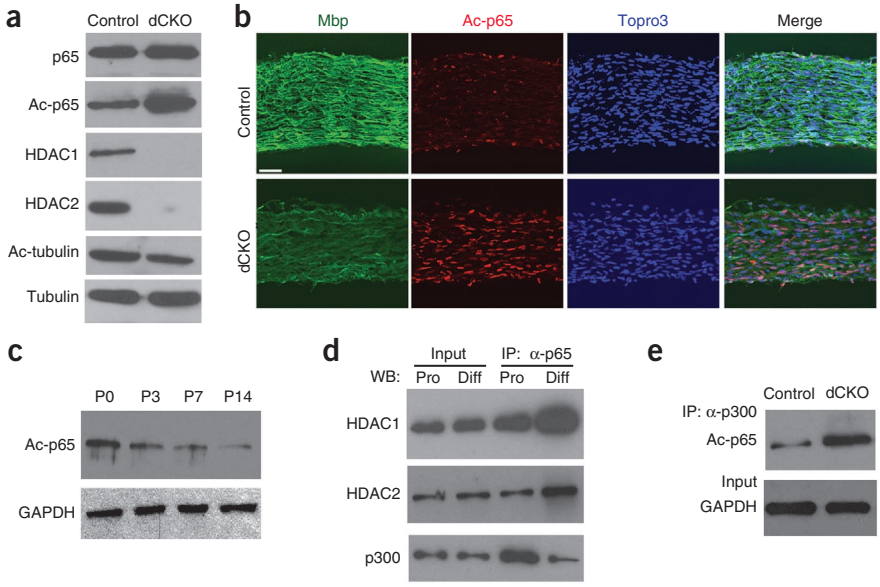

Figure 3 p65 subunit of NF-κB is an important substrate of HDAC1 and HDAC2 for Schwann cell differentiation. (**a**) Lysates of control and dCKO sciatic nerves at P4 were subject to immunoblotting analysis with antibodies to p65, acetyl-p65 K310 (Ac-p65), HDAC1, HDAC2, acetyl-tubulin (Ac-tubulin) and tubulin as indicated. (**b**) Sciatic nerves of control and dCKO mice at P4 were immunostained with antibodies to Mbp and acetyl p65. Cell nuclei were counterstained with Topro3. Scale bars represent 50 μm. (**c**) Western blot analysis of p65/RelA acetylation in wild-type sciatic nerves at P0, P3, P7 and P14 with antibodies to acetyl-p65 and GAPDH as indicated. (**d**) Lysates from primary Schwann cells under the proliferation (Pro) and differentiation (Diff) condition for 4 d were co-immunoprecipitated (IP) with antibody to p65 and blotted with antibodies to HDAC1, HDAC2, p300/CBP and GAPDH, respectively. (**e**) Lysates of control and dCKO sciatic nerves at P4 were immunoprecipitated with antibody to p300 and blotted with antibody to acetyl-p65. GAPDH was used as an input control. Full-length blots and gels are shown in **Supplementary Figure 6**.

Western blot analysis revealed that the amount of acetylated p65 markedly increased in dCKO sciatic nerves, whereas the total amount of p65 did not differ between control and dCKO at P4 (**Fig. 3a**). Consistently, we observed a robust increase in the expression intensity of acetylated p65 in dCKO sciatic nerves via immunohistochemistry (**Fig. 3b**). Acetylated tubulin levels did not increase in dCKO mice (**Fig. 3a**), suggesting that the effect of *Hdac1* and *Hdac2* deletion on p65 acetylation was specific. Similar to the lack of myelination defect, p65 acetylation levels were not altered in *Hdac1* or *Hdac2* single mutants (**Supplementary Fig. 3**).

We sought to determine the extent of p65 acetylation changes during the course of Schwann cell development and found that the amount of acetylated p65 decreased gradually from P0 to P14 (**Fig. 3c**). In addition, under the differentiation condition that promoted expression of myelination-associated proteins (**Supplementary Fig. 4**), the amount of p65 that interacted with HDAC1 and HDAC2 increased substantially in differentiating Schwann cells compared to proliferating Schwann cells (**Fig. 3d**). On the other hand, the association of p65 with p300/CBP, the major HAT for p65 acetylation[9], declined markedly in differentiating Schwann cells (**Fig. 3d**). Conversely, we observed an enhancement of acetyl p65/p300 interaction by immunoprecipitation in myelin-deficient dCKO sciatic nerves (**Fig. 3e**). Together, these results suggest that the NF-κB p65 complex stops associating with p300 and instead associates with HDAC1 and HDAC2 as Schwann cells differentiate, thereby undergoing the deacetylation process. Thus, these results identify

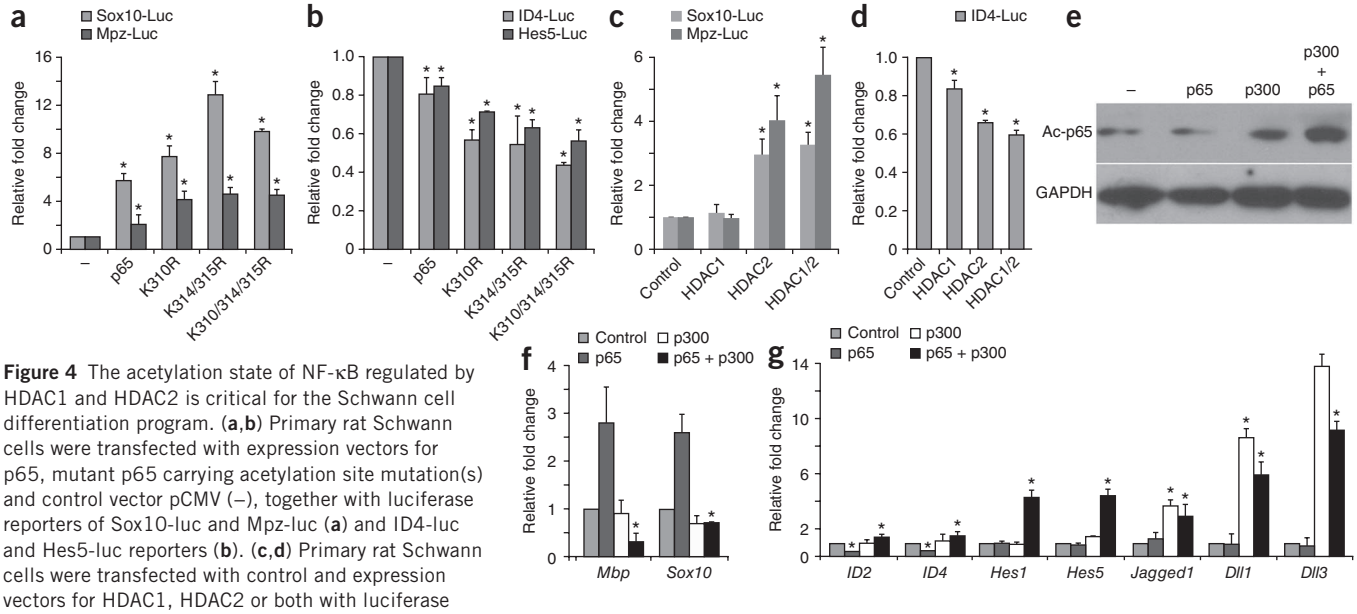

Figure 4 The acetylation state of NF-κB regulated by HDAC1 and HDAC2 is critical for the Schwann cell differentiation program. (**a**,**b**) Primary rat Schwann cells were transfected with expression vectors for p65, mutant p65 carrying acetylation site mutation(s) and control vector pCMV (–), together with luciferase reporters of Sox10-luc and Mpz-luc (**a**) and ID4-luc and Hes5-luc reporters (**b**). (**c**,**d**) Primary rat Schwann cells were transfected with control and expression vectors for HDAC1, HDAC2 or both with luciferase reporters Sox10-luc and Mpz-luc (**c**) or ID4-luc (**d**). (**e**) The lysates of primary Schwann cells transfected with expression vectors for p65 and/or p300 were immunoblotted with antibodies to acetyl-p65 and GAPDH. Full-length blots and gels are shown in **Supplementary Figure 6**. (**f**,**g**) Primary Schwann cells were transfected with expression vectors for p65, p300 or both. qRT-PCRs were performed to detect the myelination-associated genes *Mbp* and *Sox10* (**f**), as well as the differentiation inhibitors *Id2, Id4, Hes1, Hes5, Jagged1, Delta1 (Dll1)* and *Delta3* (*Dll3*) (**g**). Fold changes over controls were measured from three independent experiments in **a**–**d** and **f** and **g** ($n = 3$, $^*P < 0.01$). Error bars represent mean ± s.d.

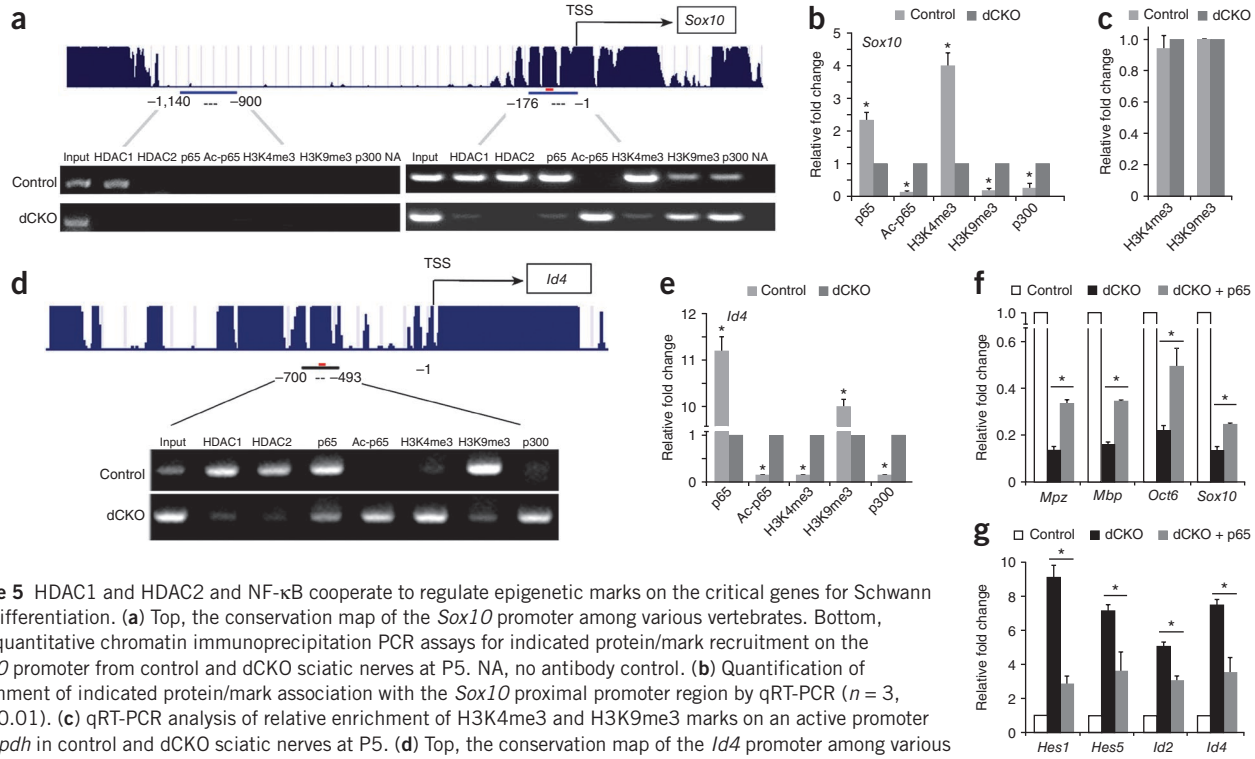

Figure 5 HDAC1 and HDAC2 and NF-κB cooperate to regulate epigenetic marks on the critical genes for Schwann cell differentiation. (**a**) Top, the conservation map of the *Sox10* promoter among various vertebrates. Bottom, semiquantitative chromatin immunoprecipitation PCR assays for indicated protein/mark recruitment on the *Sox10* promoter from control and dCKO sciatic nerves at P5. NA, no antibody control. (**b**) Quantification of enrichment of indicated protein/mark association with the *Sox10* proximal promoter region by qRT-PCR ($n = 3$, $^*P < 0.01$). (**c**) qRT-PCR analysis of relative enrichment of H3K4me3 and H3K9me3 marks on an active promoter of *Gapdh* in control and dCKO sciatic nerves at P5. (**d**) Top, the conservation map of the *Id4* promoter among various vertebrates. Bottom, ChIP PCR assays for protein recruitment on the *Id4* promoter in control and dCKO sciatic nerves at P5. (**e**) qRT-PCR for enrichment of protein/marks on the *Sox10* proximal promoter region in control and dCKO sciatic nerves. Relative fold enrichment in control versus dCKO sciatic nerves (**b**,**c**,**e**) is shown from three independent experiments ($n = 3$). The blue lines in **a** and **d** indicate PCR amplification of promoter elements with or without an NF-κB binding site (red dot) as indicated. (**f**,**g**) Primary Schwann cells isolated from dCKO sciatic nerves at P1 were transfected with control and p65 expression vectors and collected 48 h after transfection. qRT-PCR was performed to detect the myelination-associated genes *Mpz, Mbp, Oct6* and *Sox10* (**f**), as well as the differentiation inhibitory genes *Id2*, *Id4*, *Hes1* and *Hes5* (**g**) from three independent experiments ($n = 3$).

the p65 subunit of NF-κB as an important substrate of HDAC1 and HDAC2 in regulating Schwann cell differentiation.

NF-κB p65 subunit is known to be acetylated at K310, K314 and K315, whereas K310 acetylation has been reported to be critical for its transcriptional activity *in vitro*[10,11]. To determine whether the acetylation state of p65 regulates myelin gene transcription, we introduced wild-type p65 and p65 mutants carrying mutations in the acetylation sites to primary rat Schwann cells, along with reporters for differentiation activators or inhibitors. Transfection of wild-type p65 substantially transactivated reporter activities of *Sox10* or the myelin gene *Mpz* (**Fig. 4a**), while inhibiting the *Id4* or *Hes5* promoter activity (**Fig. 4b**). Overexpression of p65 acetylation mutants exhibited an enhanced ability to activate reporter activities of *Sox10* and *Mpz* promoters (**Fig. 4a**), and similarly caused a further decrease in *Id4* and *Hes5* reporter activities (**Fig. 4b**). These results suggest that the acetylation states of NF-κB p65 K310, K314 and K315 sites are involved in transcriptional control of the Schwann cell myelination program.

We next tested whether introducing HDAC1 and HDAC2 could mimic the effect of the p65 acetylation mutations in primary Schwann cells. Indeed, combination of HDAC1 and HDAC2 resulted in a 3–5-fold increase in *Sox10* and *Mpz* promoter activities (**Fig. 4c**) and a 40% reduction in *Id4* promoter activity (**Fig. 4d**). Overexpression of p300 alone increased endogenous p65 acetylation, which was further enhanced when introduced along with p65 (**Fig. 4e**). Notably, introduction of p300 substantially blocked endogenous expression of *Mbp* and *Sox10* with and without p65 in primary rat Schwann cells (**Fig. 4f**). In contrast with the positive regulators of myelination, overexpression of p300 upregulated the expression of differentiation inhibitors such as *Id2*, *Id4*, Notch effectors (*Hes1* and *Hes5*) and Notch signaling ligands (*Jagged1, Delta1* and *Delta3*)[2,3] (**Fig. 4g**). Together, these results indicate that HDAC-regulated deacetylation of NF-κB selectively activates expression of positive regulators while repressing differentiation inhibitors to promote Schwann cell myelination.

Given that HDAC1 and HDAC2 are essential for gene transcription during Schwann cell myelination, we hypothesized that the acetylation state of p65 regulated by HDACs may signal transcription-dependent changes in chromatin structure. To address the hypothesis, we performed chromatin immunoprecipitation assays with activating and repressive trimethyl histone marks, H3K4me3 and H3K9me3

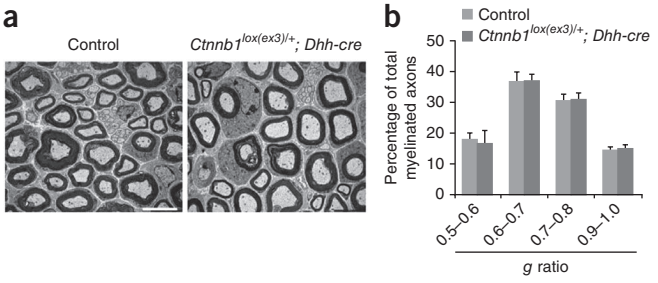

Figure 6 Activation of canonical Wnt/β-catenin signaling does not inhibit Schwann cell myelination. (**a**) Electron microscopy of sciatic nerve cross-sections from control (*Ctnnb1*$^{lox(ex3)}$) and Wnt/β-catenin activating mice in the Schwann cell lineage (*Ctnnb1*$^{lox(ex3)/+}$*; Dhh-cre*) at P15. Scale bar represents 5 μm. (**b**) The *g* ratio (ratio of axon diameter to myelinated fiber diameter) of the myelinated axons was measured in sciatic nerves of control and β-catenin activating mice. The histogram shows the percentage of counts for myelinated axons at the different ranges of *g* ratio as mean ± s.d.

(refs. 12,13), respectively, in addition to p65 and acetylated p65. As for the target genes, we chose Schwann cell regulatory genes *Sox10* and *Id4* (ref. 3), as both contained a highly conserved NF-κB binding site in their promoter regions. In particular, the *Sox10* promoter carrying the NF-κB site was shown to direct reporter gene expression in Schwann cells both *in vivo* and *in vitro*[14].

In control sciatic nerves, HDAC1, HDAC2 and p65 were recruited to the *Sox10* promoter region carrying the NF-κB binding site, but not to the region that lacked the NF-κB consensus site (**Fig. 5a**). In contrast, in dCKO sciatic nerves, p65 recruitment was hardly detectable, whereas acetyl-p65 recruitment increased markedly (**Fig. 5a**), which coincided with the increase of p300 recruitment (**Fig. 5a**,**b**). Of particular interest is that robust recruitment of an activating histone mark, H3K4me3, to the promoter region observed in control was no longer detected in dCKO. Instead, the recruitment of a repressive histone mark H3K9me3 increased significantly in dCKO (**Fig. 5a**,**b**). As a control, the recruitment level of H3K4me3 and H3K9me3 on the housekeeping gene *Gapdh* promoter was comparable between control and dCKO sciatic nerves (**Fig. 5c**).

In the *Id4* promoter, on the other hand, the repressive mark H3K9me3 was robustly recruited in control sciatic nerves and H3K4me3 recruitment was barely detectable (**Fig. 5d**). Conversely, in the absence of HDAC1 and HDAC2, H3K4me3 was strongly recruited along with acetyl-p65 and p300, whereas H3K9me3 occupancy was significantly reduced (**Fig. 5d**,**e**). Given that trimethylation on histone H3-K4 and H3-K9 are the histone modifications that are often associated with gene activation and repression[12,13], respectively, our observations suggest that HDAC1 and HDAC2 alter the acetylation state of NF-κB on the promoter region of Schwann cell regulatory genes to induce a change of chromatin configuration in coordination with transcriptional outcome. In addition, introducing p65 into Schwann cells isolated from dCKO sciatic nerves resulted in a significant increase in the expression of myelin genes and positive regulators of Schwann cell differentiation (**Fig. 5f**) and a reduction of differentiation inhibitors (**Fig. 5g**). Thus, p65 overexpression could, at least in part, rescue the defects of the Schwann cell differentiation program caused by the loss of HDAC1 and HDAC2, suggesting that p65 is a critical target of HDAC1 and HDAC2 for Schwann cell differentiation.

DISCUSSION

Requirement of HDACs for the formation of both myelinating oligodendrocytes and Schwann cells suggests that HDAC1 and HDAC2 have a conserved function in CNS and PNS myelination by regulating common differentiation activators (for example, Sox10 and YY1) and inhibitors (for example, ID4, Sox2 and Hes5)[6,15]. However, HDACs may have divergent effects on distinct signaling pathways and molecular targets in the CNS and PNS. We and others have shown previously that HDAC1 and HDAC2 regulate Wnt signaling[5], whose activation inhibits myelination and remyelination in the CNS[5,16]. Notably, activation of canonical Wnt signaling by β-catenin stabilization in the Schwann cell lineage did not affect Schwann cell myelination in β-catenin activating mice (*Ctnnb1*$^{lox(ex3)/+}$; *Dhh-cre*; **Fig. 6**). There might be a potential discrepancy regarding Wnt/β-catenin activities in Schwann cell development between our study and a companion study[17], in which HDAC1 was found to control Schwann cell survival by regulating Wnt/β-catenin signaling[17]. Although the reasons for the discrepancy are not clear, it might be a result of differences in the cellular context and timing.

In the PNS, NF-κB signaling is required for Schwann cell myelinogenesis[8]. We found that HDAC1 and HDAC2 control Schwann cell differentiation, at least in part, by modifying NF-κB acetylation state and cooperating with NF-κB. At present, the role of NF-κB signaling in CNS myelination remains unknown. Our data reveal a developmental switch in which the NF-κB p65 complex stops associating with HATs, such as p300, and begins associating with HDAC1 and HDAC2 on target promoters during Schwann cell differentiation (**Supplementary Fig. 5**). In addition, recruitment of chromatin modifiers, such as histone methyltransferases, by HDACs and their effectors, such as NF-κB, may also contribute to the specificity of target gene expression (**Supplementary Fig. 5**). Our results suggest that HDAC1, HDAC2 and NF-κB act coordinately to refine the epigenetic landscape for gene transcription that is required for Schwann cell myelination. Enhancing their activities may have therapeutic benefits for promoting myelin repair.

METHODS

Methods and any associated references are available in the online version of the paper at http://www.nature.com/natureneuroscience/.

Note: Supplementary information is available on the Nature Neuroscience website.

ACKNOWLEDGMENTS

We would like to thank D. Meijer for *Dhh-cre* mice, B. Carter and J. Chan for critical comments, and P. Casaccia for initial discussions. We thank Q. Weng and Z. Ma for technical support, O. Nakagawa and J. Chen for the p300/CBP and p65/RelA expression vectors, and R. Kageyama for the Hes5 luciferase reporter. This study was funded in part by grants from the US National Institutes of Health (NS072427) and the National Multiple Sclerosis Society (RG3978) to Q.R.L.

AUTHOR CONTRIBUTIONS

Y.C. conducted the majority of the experiments and analyzed the data. H.W. and X.X. contributed to HDAC mutant generation, phenotype analysis and biochemical assays. S.O.K., J.S. and H.A.S. provided reagents and input. M.H. provided the p65 mutant–expression vectors. K.A.N. provided CNP-Cre mice for initial phenotype observation. E.N.O. provided *loxP*-flanked HDAC1 and HDAC2 mice and inputs. Q.R.L. supervised the project, analyzed the data and wrote the manuscript.

COMPETING FINANCIAL INTERESTS

The authors declare no competing financial interests.

Published online at http://www.nature.com/natureneuroscience/.
Reprints and permissions information is available online at http://npg.nature.com/reprintsandpermissions/.

1. Suter, U. & Scherer, S.S. Disease mechanisms in inherited neuropathies. *Nat. Rev. Neurosci.* **4**, 714–726 (2003).
2. Jessen, K.R. & Mirsky, R. The origin and development of glial cells in peripheral nerves. *Nat. Rev. Neurosci.* **6**, 671–682 (2005).
3. Svaren, J. & Meijer, D. The molecular machinery of myelin gene transcription in Schwann cells. *Glia* **56**, 1541–1551 (2008).
4. Shahbazian, M.D. & Grunstein, M. Functions of site-specific histone acetylation and deacetylation. *Annu. Rev. Biochem.* **76**, 75–100 (2007).
5. Ye, F. *et al.* HDAC1 and HDAC2 regulate oligodendrocyte differentiation by disrupting the beta-catenin–TCF interaction. *Nat. Neurosci.* **12**, 829–838 (2009).
6. Shen, S. *et al.* Age-dependent epigenetic control of differentiation inhibitors is critical for remyelination efficiency. *Nat. Neurosci.* **11**, 1024–1034 (2008).
7. Jaegle, M. *et al.* The POU proteins Brn-2 and Oct-6 share important functions in Schwann cell development. *Genes Dev.* **17**, 1380–1391 (2003).
8. Nickols, J.C., Valentine, W., Kanwal, S. & Carter, B.D. Activation of the transcription factor NF-κB in Schwann cells is required for peripheral myelin formation. *Nat. Neurosci.* **6**, 161–167 (2003).
9. Calao, M., Burny, A., Quivy, V., Dekoninck, A. & Van Lint, C. A pervasive role of histone acetyltransferases and deacetylases in an NF-κB signaling code. *Trends Biochem. Sci.* **33**, 339–349 (2008).
10. Chen, L.F., Mu, Y. & Greene, W.C. Acetylation of RelA at discrete sites regulates distinct nuclear functions of NF-κB. *EMBO J.* **21**, 6539–6548 (2002).
11. Rothgiesser, K.M., Fey, M. & Hottiger, M.O. Acetylation of p65 at lysine 314 is important for late NF-κB–dependent gene expression. *BMC Genomics* **11**, 22 (2010).
12. Martin, C. & Zhang, Y. The diverse functions of histone lysine methylation. *Nat. Rev. Mol. Cell Biol.* **6**, 838–849 (2005).
13. Strahl, B.D. & Allis, C.D. The language of covalent histone modifications. *Nature* **403**, 41–45 (2000).
14. Antonellis, A. *et al.* Identification of neural crest and glial enhancers at the mouse Sox10 locus through transgenesis in zebrafish. *PLoS Genet.* **4**, e1000174 (2008).
15. He, Y. *et al.* Yy1 as a molecular link between neuregulin and transcriptional modulation of peripheral myelination. *Nat. Neurosci.* **13**, 1472–1480 (2010).
16. Fancy, S.P. *et al.* Dysregulation of the Wnt pathway inhibits timely myelination and remyelination in the mammalian CNS. *Genes Dev.* **23**, 1571–1585 (2009).
17. Jacob, C. *et al.* HDAC1 and HDAC2 control the transcriptional program of myelination and the survival of Schwann cells. *Nat. Neurosci.* published online, doi:10.1038/nn.2762 (20 March 2011).

ONLINE METHODS

Generation of mice with HDAC1/2 mutant mice in the Schwann cell lineage. Mice carrying the *Hdac1* and *Hdac2 loxP*-flanked alleles were bred with the *Dhh-cre* line[7], which expresses Cre in cells of the Schwann cell lineage, to generate $Hdac1^{loxP/loxP}$; *Dhh-cre*, $Hdac2^{loxP/loxP}$; *Dhh-cre*, $Hdac1^{loxP/loxP}$; $Hdac2^{loxP/loxP}$; *Dhh-cre* and control heterozygous $Hdac1^{loxP/+}$; $Hdac2^{loxP/+}$; *Dhh-cre* offspring. There was no difference in the development and behavior of control and age-matched wild-type mice. As *Hdac1* and *Hdac2* single mutant phenotypes were indistinguishable from heterozygous control, we mainly focused on the control ($Hdac1^{loxP/+}$; $Hdac2^{loxP/+}$; *Dhh-cre*) and dCKO for subsequent analyses. Conditional β-catenin activation mice were generated by breeding $Ctnnb1^{lox(ex3)}$ mice[5,18] with the *Dhh-cre* line to generate control ($Ctnnb1^{lox(ex3)/+}$) and β-catenin activating mice ($Ctnnb1^{lox(ex3)/+}$; *Dhh-cre*), in which β-catenin is stabilized in the Schwann cell lineage. Cre-mediated excision of the exon 3 of the β-catenin allele produces a shortened, stable form of β-catenin that lacks its N-terminal phosphorylation and ubiquitination sites, resulting in constitutive activation of canonical Wnt signaling in the Schwann cell lineage. Animal use and studies were approved by the Institutional Animal Care and Use Committee of the University of Texas Southwestern Medical Center at Dallas.

Immunohistochemistry, electron microscopy and western blot analysis. Sciatic nerves were fixed in 4% paraformaldehyde (wt/vol) for 10 min, and then were embedded in optimal cutting temperature media, cut into 10-μm cross or longitudinal sections. For BrdU pulse labeling, animals were injected intraperitoneally on P4 with 100 mg per kg of body weight BrdU 2 h before sciatic nerve collection. For primary antibodies, we used mouse antibodies to Mbp, Mpz and Mag (Covance), rabbit antibody to Krox20/Egr2 (Covance), goat antibody to Oct6 (Santa Cruz), goat antibody to Sox10 (Abcam), mouse antibody to BrdU (BD Biosciences), rabbit antibody to Ki67 (Thermo Scientific), rabbit antibody to caspase 3 (Millipore), antibody to p300/CBP (Santa Cruz), antibody to NF-κB p65/RelA (Santa Cruz) and antibody to acetylated NF-κB p65 (acetyl K310, Abcam). The acetyl-p65 antibody detected NF-κB p65 acetylation at K310, the major acetylation site in p65. Currently, the antibodies for NF-κB acetylated at K314 and K315 are not commercially available. Topro3 (Molecular Probes) was used for a cell nuclei stain. All images were acquired using a Zeiss LSM 510 confocal microscope. For electron microscopy, sciatic nerves were dissected and fixed in fixative solution containing 2% paraformaldehyde, 2% glutaraldehyde (vol/vol) and 0.1 M cacodylic acid (pH 7.2) and processed for electron microscopy. Western blot analysis was performed according to the method described previously[19]. GAPDH or tubulin was used as an input control.

qRT-PCR. qRT-PCR was carried out using the ABI Prism 7700 Sequence Detector System (Perkin-Elmer Applied Biosystems) using *Gapdh* (TaqMan kit, Applied Biosystems) as an internal control as previously described[5]. qPCR primers for mouse species: *Mpz* (forward, CTG GTC CAG TGA ATG GTC T; reverse, GTC CCT TGG CAT AGT GGA AA), *Mbp* (forward, TCA CAG AAG AGA CCC TCA CA; reverse, GCC GTA GTG GGT AGT TCT TG), *Oct6* (forward, GTT CTC GCA GAC CAC CAT CT; reverse, GTC TCC TCC AGC CAC TTG TT), *Sox10* (forward, AGC CCA GGT GAA GAC AGA GA; reverse, GTC AAA CTG GGG TCG TGA G), *Hes1* (forward, TCT GGA AAT GAC TGT GAA CA; reverse, GTC ACC TCG TTC ATG CAC TC), *Hes5* (forward, AGC TAC CTG AAA CAC AGC AAA GCC; reverse, TAA AGC AGC TTC ATC TGC GTG TCG), *Id2* (forward, TGA ACG ACT GCT ACT CCA AGC TCA; reverse, GTG CTG CAG GAT TTC CAT CTT GGT), *Id4* (forward, GCA GTG CGA TAT GAA CGA CTG CTA; reverse, TAA CGT GCT GCA GGA TCT CCA CTT), *Gpr126* (forward, TTA TGT GAG CTG TGC CGG GTA CTT; reverse, ATT CCT CCC ACA GAT CTG CAC CAT), *Gjb1* (forward, TTC AGA ATC ATG GTG CTG GTG GTG; reverse, ACC AAG ATA AGC TGC AGG GAC CAT), *Krox20* (forward, CAG GAG TGA CGA AAG GAA GC; reverse, ACC AGA GGC TGA AGA CTG G), *Sox2* (forward, CAC AAC TCG GAG ATC AGC AA; reverse, CTC CGG GAA GCG TGT ACT TA), *Sox11* (forward, GCT GGA AGA TGC TGA AGG AC; reverse, GTC GGG ATA ATC AGC CAT GT), *Jun* (forward, ACC CCC ACT CAG TTC TTG TG; reverse, AGT TGC TGA GGT TGG CGT AG) and *Jagged1* (forward, CAA ATG AGT GCG AGG CCA AAC CTT; reverse, AGC CAG GAA GGC AAT CAC AGT AGT).

qPCR primers for rat species: *Mbp* (forward, TTG ACT CCA TCG GGC GCT TCT TTA; reverse, GCT GTG CCA CAT GTA CAA GGA TCA), *Sox10* (forward, GCT ATC CAG GCT CAC TAC AAG; reverse, ACT GCA GCT CTG TCT TTG G), *Id2* (forward, ATG GAA ATC CTG CAG CAC GTC ATC; reverse, ACG TTT GGT TCT GTC CAG GTC TCT), *Id4* (forward, ACT GTG CCT GCA GTG CGA TAT GAA; reverse, TGC AGG ATC TCC ACT TTG CTG ACT), *Hes1* (forward, AGA AAA ATT CCT CGT CCC CG; reverse, TTT CAT TTA TTC TTG CCC GGC), *Hes5* (forward, ACC AGC CCA ACT CCA AAC; reverse, AGT AAC CCT CGC TGT AGT CC), *Jagged1* (forward, GAC TAC GAG GGC AAG AAC TG; reverse, GTT GGA AGA GAT ATA CCG CAC C), *Dll1* (forward, TTC TCT GGC TTC AAC TGT GAG; reverse, TCA TCC ACA TTG TCC TCG C) and *Dll3* (forward, ATT CTA TGG GCC TCG ATG TGA GGT; reverse, AGG ATC TTC ACC GCC AAC ACA CAA).

Primary Schwann cell culture and transfection. Rat Schwann cells were prepared from sciatic nerves of newborn rats (1–2 d old) as described previously[20]. For routine culture, rat Schwann cells were grown under the proliferation condition (DMEM (Gibco) with 10% fetal bovine serum (vol/vol, Hyclone) supplemented with 10 ng ml^{-1} neuregulin (R&D) and 5 μM forskolin (Sigma-Aldrich)). Cells between passages 2 and 4 were used in all experiments. To promote differentiation, Schwann cells were cultured in a differentiation medium (DMEM with N2 (Gibco) supplemented with 5 μM forskolin), resulting in a substantial increase of expression of differentiation markers, including Mpz and Krox20. Primary mouse Schwann cells were prepared from sciatic nerves of newborn mice (P1) as described previously[21] and cultured on poly-D-lysine (Sigma) coated plates in DMEM (Gibco) with 10% FBS (Hyclone) supplemented with 50 ng ml^{-1} beta heregulin (EGF domain) (R&D Systems). The primary Schwann cells were greater than 95% pure and used for transfection study after isolation. For reporter assays, rat Schwann cells were transfected with luciferase reporters and expression vectors using Lipofectamine 2000 (Invitrogen). Transfected cells were cultured for 48 h before collecting to measure the luciferase activity using luciferase assay kit (Promega). The pRSV-renilla luciferase plasmid was included to control for variable transfection efficiencies between different experiments ($n \geq 3$ times).

Chromatin immunoprecipitation (ChIP) assays. ChIP assay was performed as described[19]. Briefly, sciatic nerves were dissected from control and HDAC mutant mice and immediately fixed in 1% formaldehyde (wt/vol) for 25 min at 22–23 °C. Nerves were washed in phosphate-buffered saline, homogenized in 150 mM NaCl, 10% glycerol (vol/vol), 0.3% Triton X-100 (vol/vol) and 50 mM Tris-HCl (pH 8.0) containing protease inhibitor cocktail (Roche) as described previously[22]. Lysates were then sonicated with a Bioruptor sonicator (Diagenode) to ~500 bp. Sheared chromatin (~30 μg) was incubated with 2 μg of antibody to HDAC1, HDAC2, p65, acetylated p65 K310, trimethyl-histone3 K4 (Abcam), trimethyl-histone3 K9 (Abcam) and p300 (Abcam) for each ChIP assay. Real-time PCR was carried out using quantitative SYBR green PCR mix (Applied Biosystems). The relative fold enrichments were determined by the $2^{-\Delta CT}$ methods as previously described[23]. Samples were normalized to input chromatin. Primers used for ChIP-PCR analysis: *Sox10* proximal promoter (−1/−176; forward, AGG CAG CAG TGC GGG TCA CA; reverse, TGA CTG AGC CGC TGC AGA CG), *Sox10* 5′ UTR (−900/−1,140; forward, AAT CAT TGA GGC CTT GAT TC; reverse, CTC TAC AGC CTA GTT AGT GT), *Id4* promoter (−700/−493; forward, ATT CCA GCC AGC ACA TTC C; reverse, GGA GTG ACC AGC CAA TCA G) and *Gapdh* proximal promoter (forward, TTT GAA ATG TGC ACG CAC CAA GCG; reverse, TGA GTC CTA TCC TGG GAA CCA TCA).

Statistic analysis. Quantifications were performed from at least three experimental groups. Data are presented as mean ± s.d. in the graphs. *P* values are from Student's two-tailed *t* test to compare two sets of data. $P < 0.05$ is considered to be statistically significant.

18. Harada, N. *et al.* Intestinal polyposis in mice with a dominant stable mutation of the beta-catenin gene. *EMBO J.* **18**, 5931–5942 (1999).
19. Chen, Y. *et al.* The oligodendrocyte-specific G protein–coupled receptor GPR17 is a cell-intrinsic timer of myelination. *Nat. Neurosci.* **12**, 1398–1406 (2009).
20. Brockes, J.P., Fields, K.L. & Raff, M.C. Studies on cultured rat Schwann cells. I. Establishment of purified populations from cultures of peripheral nerve. *Brain Res.* **165**, 105–118 (1979).
21. Yeiser, E.C., Rutkoski, N.J., Naito, A., Inoue, J. & Carter, B.D. Neurotrophin signaling through the p75 receptor is deficient in $traf6^{-/-}$ mice. *J. Neurosci.* **24**, 10521–10529 (2004).
22. Jang, S.W., LeBlanc, S.E., Roopra, A., Wrabetz, L. & Svaren, J. *In vivo* detection of Egr2 binding to target genes during peripheral nerve myelination. *J. Neurochem.* **98**, 1678–1687 (2006).
23. Bernstein, B.E. *et al.* A bivalent chromatin structure marks key developmental genes in embryonic stem cells. *Cell* **125**, 315–326 (2006).

doi:10.1038/nn.2780